



Heterogeneous and homogeneous nucleation of Taxol™ crystals in aqueous solutions and gels: Effect of tubulin proteins

Javier S. Castro^{a,c,*}, Pierre A. Deymier^a, Bartosz Trzaskowski^{b,1}, Jaim Bucay^a

^a Department of Materials Science and Engineering, University of Arizona, Tucson, AZ 85721, United States

^b Department of Chemistry, University of Arizona, Tucson, AZ 85721, United States

^c Autonomous University of Juarez City (UACJ), Juarez City, Chih, Mexico 32310, Mexico

ARTICLE INFO

Article history:

Received 7 April 2009

Received in revised form 21 October 2009

Accepted 21 October 2009

Available online 31 October 2009

Keywords:

Taxol

Paclitaxel

Crystals

Spherulites

Tubulin

Nucleation

Microtubule aster

ABSTRACT

In this study we report crystallization of Taxol in pure water, aqueous solutions containing tubulin proteins and tubulin-containing agarose gels. We show that crystallization of Taxol in tubulin-free aqueous solutions occurs by the formation of sheaf-like crystals, while in the presence of tubulin Taxol crystallizes in the form of spherulites. Whereas sheaves are characteristic for crystals formed by homogeneous nucleation, the spherical symmetry of the Taxol crystal formed in the presence of tubulin suggests they result from heterogeneous nucleation. To explain the formation of tubulin–Taxol nuclei we suggest a new, secondary Taxol-binding site within the tubulin heterodimer. Contrary to the known binding site, where the Taxol molecule is almost completely buried in the protein, the Taxol molecule in the secondary binding site is partially exposed to the solution and may serve as a bridge, connecting other Taxol molecules. Results presented in this work are important for *in vivo* and *in vitro* microtubule studies due to the possibility of mistaking these Taxol spherulites for microtubule asters, moreover a novel variable is proposed in the study of cells treated with Taxol for cancer treatment via sequestration of tubulin.

© 2009 Elsevier B.V. All rights reserved.

1. Introduction

To date Taxol™ (paclitaxel) has been demonstrated to be one of the most effective drugs in the treatment of a variety of cancers [1,2]. In the cytoplasm, Taxol binds to polymerized tubulin at a specific tubulin–Taxol binding site stabilizing microtubules (MTs). Stabilization of spindle MTs blocks eukaryotic cell division (mitosis) [3–5] arresting the growth of tumors. Despite the vast amount of research already done on this drug during the past three decades, there is still a huge interest in understanding its properties, behavior and interaction with tubulin and other molecules.

One of the main challenges in Taxol-based *in vivo* treatments is its poor solubility. In order to overcome this problem it has been necessary to use delivery vehicles that may cause allergic reactions in the body [6,7]. On the other hand, *in vitro* studies have shown that Taxol may induce the growth of MT asters in cells treated with this drug [8–12]. Since the detection of MT asters is usually performed by immunolabeling followed by fluorescent microscopy analysis,

Foss et al. noticed recently that some of these MT asters could be, in fact, Taxol crystals decorated with fluorescent tubulin, mimicking MTs asters [13]. This hypothesis is also supported by our recent observations of high binding affinity of various fluorochromes to Taxol crystals [14]. Moreover, in that same paper, based on semi-empirical docking modeling approaches, we proposed a new potential Taxol-binding site in the tubulin heterodimer. As will be seen in the current report, this hypothesis is strengthened by evidences of heterogeneous nucleation of Taxol crystals by tubulin heterodimers. These evidences are consistent with the existence of the secondary Taxol-binding site. These results strengthen Foss et al.'s proposed mechanism that Taxol crystals can sequester tubulin heterodimers. However, our data suggest that sequestration occurs by tubulin's ability to nucleate crystals rather than by laterally decorating them, as proposed in [13]. This sequestration mechanism could add to our understanding of how cells in a cancer patient respond to treatment with Taxol (paclitaxel).

Taxol spherulitic growth has been rarely reported in literature [6,15], and little details have been provided concerning this interesting phenomenon. Nevertheless spherulitic crystallization has been widely studied in other materials. In polymers, where this phenomenon is commonly observed, spherulites form during supercooling of the melted polymer. Spherulitic growth is also found in inorganic crystals such as mesolite, scolecite, and natrolite; in proteins such as lysozyme [16,17], β -lactoglobulin and insulin [18]; and in organic crystals such as aspartame [19].

* Corresponding author at: 1235 E. James E. Rogers way, Tucson, AZ 85721, United States. Tel.: +1 520 621 6070; fax: +1 520 621 8059.

E-mail addresses: jscastro@email.arizona.edu, javiercastro8@hotmail.com (J.S. Castro).

¹ Current address: Materials and Process Simulation Center, California Institute of Technology, Pasadena, CA 91125, United States.

Spherulitic growth occurs when crystallization is carried out in an isotropic three-dimensional medium and it is initiated from a nucleation process that can be homogeneous or heterogeneous. Each nucleation mechanism produces a different structure [20]. Homogeneous nucleation begins from a single needle-like crystal that grows axially and branches out forming sheaf-like aggregates also called axialites. When a large number of axialite's arms form, the system takes on a spherulitic appearance. On the other hand heterogeneous nucleation starts from a foreign particle that leads to very symmetric star-shaped spherulites with needle-like crystals radiating in three dimensions.

The formation of needle-like crystals can be explained by an anisotropic growth in which certain faces of the crystal grow much faster than others, leading to elongated crystals. The fast growth on the top face of the elongated crystal is usually attributed to a two-dimensional nucleation which produces a roughened surface. The growth is controlled by supply of the material to the roughened face, a phenomenon known as kinetic roughening [21]. The reason for the slower growth of lateral faces is unclear. It has been suggested that this process occurs via layer-by-layer growth, which is more difficult than the 2D nucleation on the top faces [22]. Computational models of aspartame spherulites have shown that top faces start to grow at low driving forces, whereas the more stable lateral faces grow at much higher driving forces [19]. Hence, at supersaturation conditions, the top faces will grow rapidly, while lateral faces will grow slowly producing a needle-like morphology.

Our present study reports on an investigation of the effect of tubulin on the morphology of Taxol crystals grown in aqueous liquid environments as well as in water-based agarose gels. Because most Taxol applications take place in the cytoplasm, where Taxol interacts with tubulin, we studied Taxol crystals formation in tubulin-containing aqueous solutions. We also considered tubulin-containing agarose gels to mimic the gel-like nature of the cytoplasm. Through the investigation of the morphology of the Taxol crystals, we aim at shedding more light on the nature of the nucleation processes that lead to crystallization. The experimental observations show that Taxol nucleates heterogeneously in the presence of tubulin forming spherically symmetric star-like spherulites. In absence of tubulin, Taxol forms homogeneously nucleated sheaves. To explain the heterogeneous nucleation of Taxol asters, we propose the formation of Taxol–tubulin dimer complexes via a secondary Taxol–tubulin binding site, reported previously.

2. Results and discussion

2.1. Crystallization of Taxol in aqueous liquid environments

We first studied the formation of Taxol crystals in pure water. For this purpose, a supersaturated Taxol solution was prepared using filtered deionized water and Taxol (dissolved in DMSO) 100 μM concentration. Due to the fact that Taxol crystals are transparent, we used differential interference contrast (DIC) microscopy to analyze samples from this solution, to find that Taxol aggregates with axialite-like shapes (Fig. 1a).

Since Taxol interacts with tubulin in the cytoplasm, we also investigated Taxol crystals formation in tubulin-containing aqueous solutions. For this step we used a MT supporting buffer containing tubulin (9.1 μM) to which Taxol was added at a concentration of 100 μM . Taxol structures obtained in this experiment showed significant morphological differences to those grown in pure water, when analyzed by DIC microscopy. Structures from this solution displayed spherulitic shapes with larger diameters and lower number density (Fig. 1b) compared to axialites obtained in pure water. Besides the buffer and tubulin, no other changes

in the protocol were implemented, so all the morphological differences between these two experiments can be attributed exclusively to the addition of some heterogeneities, such as salts contained in the MT supporting buffer or the tubulin. To discard the effect of the buffer in spherulites formation we performed a control experiment where Taxol crystals were grown in a MT supporting buffer, but without the presence of tubulin. In this control study we obtained axialites similar to those grown in pure water (image not shown here). This observation confirms that tubulin and not the buffer constituents give rise to the nucleation and growth of Taxol spherulites.

In the next step we have considered using immunolabeling as a method to investigate the presence of tubulin in the center of Taxol spherulites. Unfortunately, due to the high affinity of fluorescent conjugated molecules to Taxol crystals [14], it is impossible to differentiate Taxol from tubulin in this type of studies. Due to this problem we performed some alternative experiments to find whether tubulin is located in the center of Taxol spherulites.

We used rhodamine to label spherulites previously formed in buffer solution containing regular tubulin. Prior to this experiment we have verified experimentally that rhodamine does not bind to tubulin nor MTs under our experimental conditions, but it binds to Taxol crystals in the prepared solution. Images of this solution with fluorescent microscopy (Fig. 1c) show fluorescent spherulites with morphologies similar to those produced in the presence of tubulin and viewed with DIC (Fig. 1b). We noted, however, the lack of fluorescence in the centers of many spherulites. This absence of fluorescence indicated that Taxol is not available for binding to the fluorochrome and strongly suggests the presence of tubulin in the core of spherulites.

Looking for a better method of tubulin detection in the spherulites, we used a fluorescent-labeled tubulin (rhodamine tubulin) to nucleate Taxol crystals. One advantage of this method is the fact, that spherulites grown in the presence of rhodamine tubulin are automatically labeled with the fluorescent conjugated molecule due to the rhodamine tag binds to the surface of Taxol crystals [14]. This method enables us to use fluorescence microscopy to image these structures, eliminating the rhodamine labeling step. In this sample (Fig. 1d) we observed fluorescent spherulites with morphologies similar to those seen in the experiment performed with regular tubulin. In these images, the center of the spherulites appeared completely illuminated by fluorescence, which may indicate the presence of fluorescent tubulin in the core, although it could also result from the higher density of Taxol sites in the core of the spherulite that can interact with rhodamine tubulin.

In order to explore further the role of rhodamine in nucleation of Taxol spherulites, we conducted a control experiment to study the growth of Taxol crystals in the presence of pure rhodamine. For this study, we used a rhodamine-containing solution into which Taxol was added. The structures obtained in this study (Fig. 1e) were fluorescent axialites morphologically similar to those grown in pure water, indicating that pure rhodamine does not nucleate Taxol spherulites.

Besides the effect of nucleation in Taxol spherulites, we also explored the impact of tubulin on the growth of Taxol crystals after nucleation in a tubulin-free aqueous solution. We prepared a supersaturated Taxol solution in MT supporting buffer, to initiate the nucleation, and after 10 s rhodamine tubulin was added. Previously we had verified by means of DIC microscopy, using similar Taxol concentrations that Taxol axialites nucleate immediately after Taxol is diluted in aqueous solutions. We obtained fluorescent axialites (Fig. 1f), which allows us to suggest that after nucleation tubulin does not interfere with Taxol crystals growth.

Under our experimental conditions Taxol crystals were nucleated quickly and reached their quasi-equilibrium state within approximately fifteen minutes. Samples containing Taxol crystals

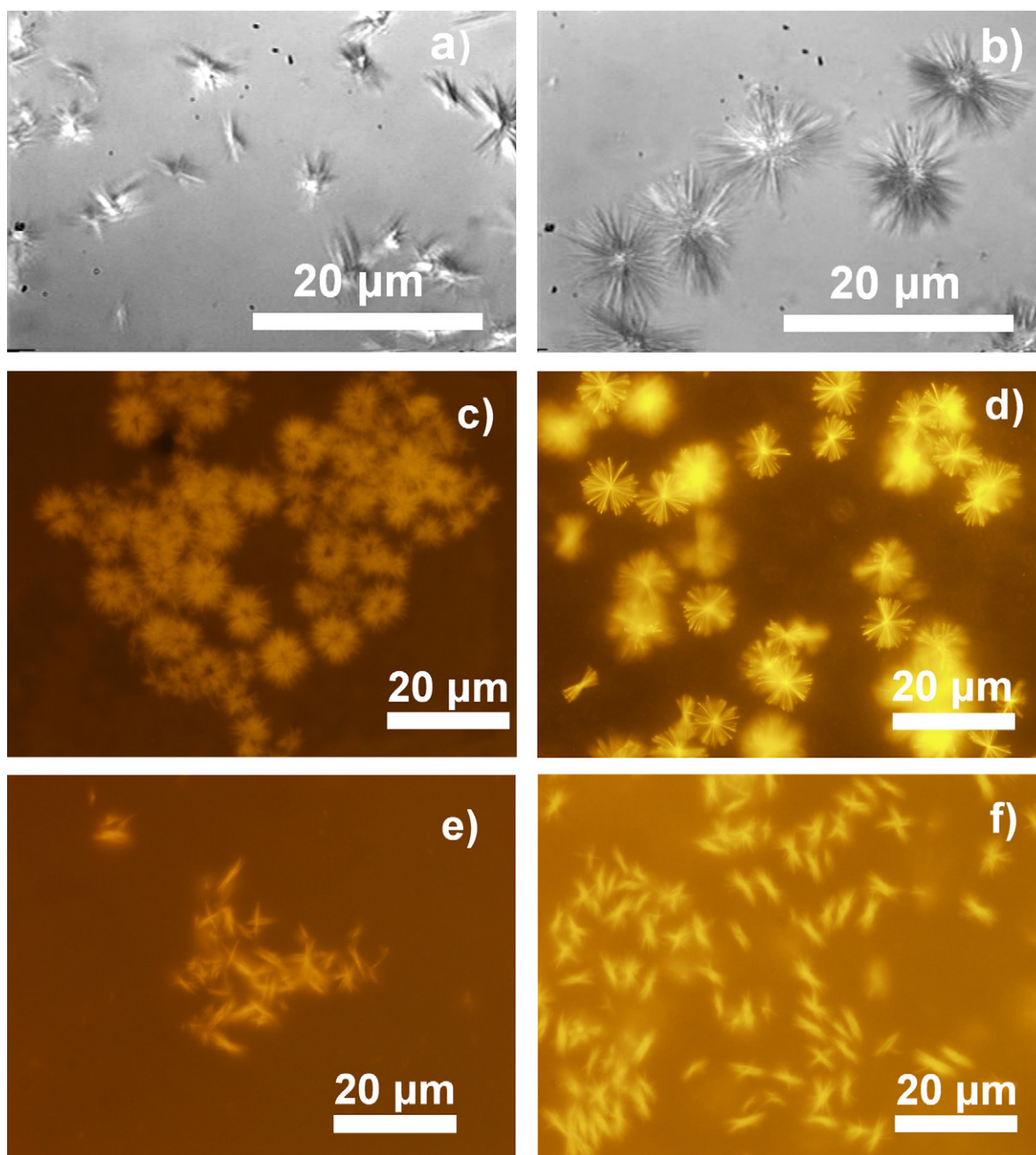


Fig. 1. Taxol crystallization in various aqueous solutions. (a) Differential Interference contrast (DIC) microscopy image of axialites formed in a tubulin-free solution. (b) DIC image of spherulites formed in the presence of pure tubulin. (c) Fluorescence microscopy image of spherulites formed in the presence of pure tubulin with rhodamine added after growth. Subsequent images are taken with fluorescent microscopy. (d) Spherulites formed in the presence of rhodamine tubulin. (e) Axialites formed in the presence of rhodamine. (f) Axialites nucleated in a free-tubulin solution with rhodamine tubulin added during growth.

stored for 24 h at room temperature did not show any noticeable morphological changes. We noted that crystals' sizes (defined by average diameter) and number of crystals in the solution can be strongly affected by Taxol concentration and temperature, thus in all these experiments Taxol concentration, temperature, and incubation time were fixed. We also observed that these variables did not affect Taxol crystals' shapes (i.e. sheaf-like or spherulitic), which were defined by their nucleation process.

We did not observe branched needles, yet we observed quite uniform distribution of needles lengths for each crystal. Due to this fact we discarded the possibility of secondary nucleation, since late nucleation would form a very distinctive bimodal distribution of needle lengths.

2.2. Effect of tubulin concentration on crystallization of Taxol in aqueous liquid environments

To clarify the role of tubulin in the nucleation of Taxol spherulites we investigated the effect of the concentration of rhodamine tubulin on the crystallization of Taxol in buffer solutions. We used three rhodamine tubulin-containing solutions with tubulin concentrations of 0.9, 9.1 and 27 μM , named solution A, B, and C, respectively. In these solutions Taxol concentration was 100 μM . We report the images of these solutions in Fig. 2. At low tubulin concentration (solution A) we may observe some Taxol spherulites (Fig. 2a), although Taxol appears to crystallize predominantly in the form of axialites (Fig. 2b). We also note that

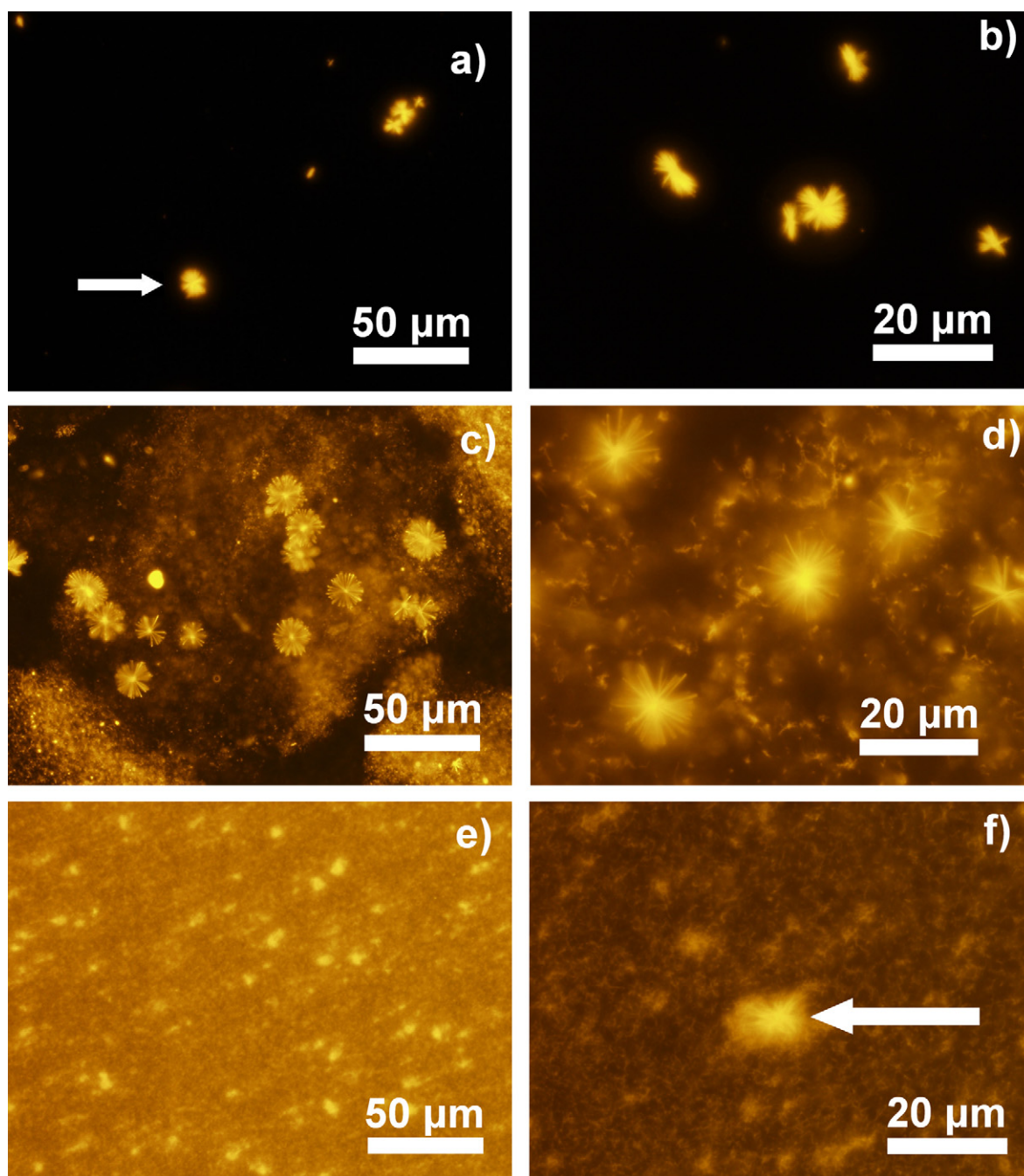


Fig. 2. Effect of rhodamine tubulin concentration on Taxol crystallization. Three solutions were prepared with a fixed Taxol amount ($100\ \mu\text{M}$) but different rhodamine tubulin concentrations as follow: solution A with $0.9\ \mu\text{M}$, solution B with $9.1\ \mu\text{M}$, and solution C with $27\ \mu\text{M}$. (a) and (b) are images from solution A taken at $40\times$ and $100\times$ magnifications respectively. Axialites and a spherulite (arrow) are observed. Neither MTs nor free rhodamine tubulin were noted in the background. (c) and (d) are images from solution B where spherulites and a background composed of short MTs and probably unpolymerized rhodamine tubulin are observed. Finally, (e) and (f) are images from solution C. Short MTs and bright spots are predominantly observed. The arrow shows a Taxol crystal surrounded by a fluorescent halo, probably made of small MTs. Numerous MTs are observed in the background. All images were taken with fluorescent microscopy.

images do not show any evidence of MTs formation. The solution B, with tubulin concentration of $9.1\ \mu\text{M}$, was used in the experiments reported in the previous section. The results (Fig. 2c and d) show mostly Taxol spherulites and some MTs. In the solution C, containing the high tubulin concentration ($27\ \mu\text{M}$), few Taxol crystals (mostly axialites) were found in the sample, but a dense background of short microtubules and bright spots was observed (Fig. 2e and f). To understand these results it is necessary to note that rhodamine tubulin has three distinct functions that are revealed by these experiments, namely (a) to form heterogeneous Taxol nuclei, (b) to label Taxol crystals and, (c) to form

MTs. In the case of low tubulin concentration the tubulin available to generate heterogeneous nuclei is very low compared to the relatively high Taxol concentration, leading to the coexistence of numerous homogeneously nucleated axialites and a few heterogeneously nucleated spherulites. Moreover, the absence of MTs in the image indicates that nucleation and labeling have rapidly depleted the solution of rhodamine tubulin, making it unavailable for growing MTs. At the intermediate tubulin concentration there is enough tubulin to nucleate and label spherulites, as well as to make some MTs. Finally, in the case of the high tubulin concentration (solution C) the small number of Taxol crystals contrasts

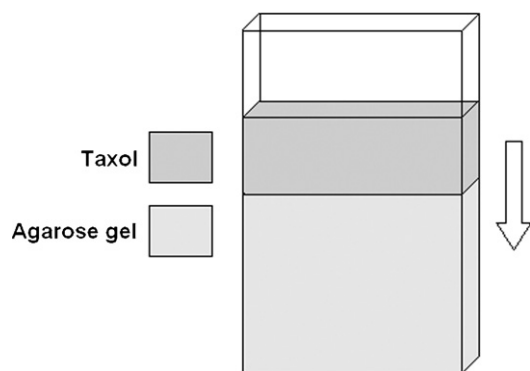


Fig. 3. Taxol crystallization in solid agarose gels via diffusion. Taxol diffusion in a rectangular column (5 mm × 1.5 mm × 10 mm) with optically transparent walls. The large volume of Taxol produces a nearly continuous Taxol supply. Arrow indicates the direction of Taxol diffusion.

with the large amount of MTs and bright spots observed in the sample.

This later observation suggests that in the solution C the high tubulin concentration triggered the fast growth of MTs, depleting tubulin heterodimers from the solution. MTs consumed approximately 27% of the Taxol molecules for their stabilization. The remaining Taxol (73%) was available to form crystals. However, this value is significantly lower than a 99% in solution A and a 91% in solution B. Hence, the driving force for Taxol crystallization was considerably reduced producing fewer and smaller crystals. Small crystals could trap MTs between their needles producing clusters of MTs that could appear as bright spots as shown in Fig. 2e and f. In conclusion, the different morphologies encountered in samples containing identical concentrations of Taxol but different tubulin concentrations are suggestive of a key role of tubulin in nucleation of Taxol crystals.

2.3. Crystallization of Taxol in agarose gels

In this part of our investigation we analyzed the crystallization of Taxol in tubulin-containing agarose gels, an analog of the cell cytoplasm. These rich tubulin-containing gels may be seen as models to simulate the gel-like, crowded environment in the cytoplasm, where Taxol is used for MTs stabilization. Also, it is worth noting that these experiments utilized Taxol diffusion into agarose gels, which is similar to Taxol diffusion in cytoplasm. We selected agarose because it is both electrically and chemically neutral and does not interact with tubulin nor with MTs [23]. To support the gel we used a rectangular cuvette with optically transparent side walls (Fig. 3).

In the column, 20 μ L of rhodamine tubulin-containing gel was solidified and 15 μ L of Taxol in DMSO at 2 mM concentration was deposited over the solid gel. This setting allowed Taxol diffusion through the gel, providing a continuous supply of Taxol. The sample was analyzed through the transparent walls observing fluorescent spherulites with large diameters (Fig. 4a). The large diameters of these spherulites can be attributed to a high local concentration and a continuous, but slow Taxol supply, generating a continuous growth, until Taxol was depleted. The large size of these spherulites allowed us to better analyze their morphology, observing very bright and well defined cores and Taxol needles pointing radially. Repeating this experiment with pure rhodamine instead of fluorescent tubulin yielded axialites with large diameters lacking a defined center (Fig. 4b).

These experimental results reinforce our observation that heterogeneous nucleation of Taxol crystals is initiated by tubulin. The unequivocal morphological differences between spherulites and

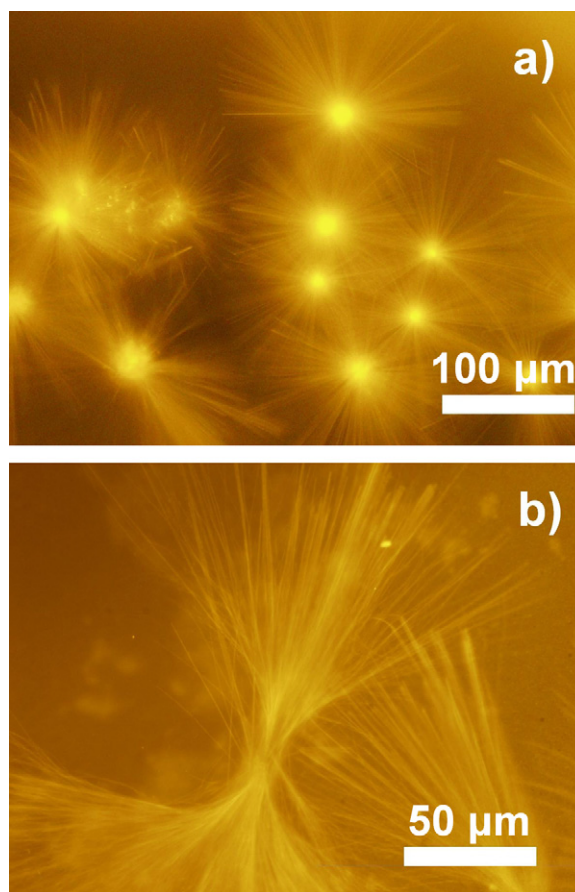


Fig. 4. Taxol crystals grown in solid agarose gels through a continuous supply of Taxol. (a) Spherulites grown in a rhodamine tubulin-containing agarose gel. (b) Axialites grown in a rhodamine (tubulin-free) agarose gel.

axialites can only be attributed to the presence of tubulin. This result suggests that tubulin can interact with Taxol in a manner that can lead to the heterogeneous nucleation of Taxol spherulites. Moreover, the well defined and bright cores indicate the presence of rhodamine tubulin in the centers of spherulites. On the other hand, the branching of axialites from needles located in the axial center indicates the nucleation and growth of these structures from needles made of the same material, demonstrating the homogeneous nucleation in the absence of tubulin.

2.4. Taxol–tubulin binding site

To provide a plausible explanation for the nucleation of Taxol crystals from tubulin it is necessary to analyze the interactions found in Taxol crystals as well as between tubulin and Taxol. The crystal structure of tubulin dimer reveals that a primary Taxol-binding site is located in a hydrophobic pocket of β -tubulin [24]. The Taxol molecule (Fig. 5a) is buried deeply into this pocket, interacting with a number of hydrophobic residues including Leu 217, Ala 233, His 229, Leu 275, Gly 370 and Leu 371. Moreover, all Taxol atoms important for the formation of Taxol crystals (which include O1 hydroxyl oxygen, C2 benzoyl oxygen, O2' hydroxyl oxygen, C5' carbonyl oxygen, O7 hydroxyl oxygen and C10 acetyl oxygen) are also buried inside the binding pocket (Fig. 5b) and not able to form hydrogen bonds with another Taxol molecule to form a crystal structure [25]. As a result of this simple analysis we can exclude this binding site as being responsible for nucleation of Taxol crystals from tubulin.

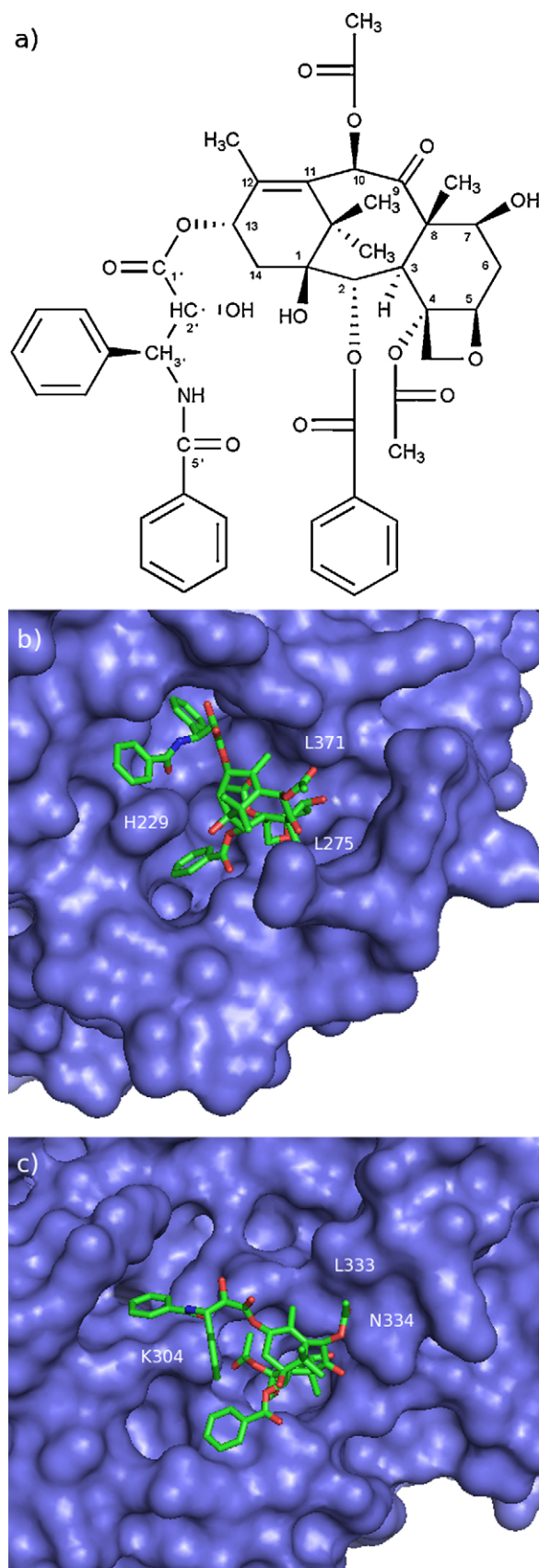


Fig. 5. Details of Taxol structure and Taxol-binding sites within tubulin dimer. (a) Schematic representation of Taxol molecule and atom numbering used in this work. (b) The native Taxol-binding site in the beta-tubulin monomer. (c) The new candidate for Taxol-binding site in the groove between alpha-tubulin and beta-tubulin monomers.

In our previous work we have suggested that there may exist another Taxol-binding site within the tubulin dimer [14]. Computational analysis of the tubulin–Taxol system using docking methods allowed us to propose a potential binding site, different from the site identified by X-ray analysis. The new binding site is located in the outer surface of the MT in a small groove on the boundary between α and β tubulin monomers and the main residues involved in interactions with Taxol are Gln 176, Arg 214, Lys 304, Leu 333 and Asn 334. The most important difference between the two binding sites is the fact that in the case of new binding site the Taxol molecule is only partially buried in the bonding pocket, exposing some parts of the molecule to the solvent. Specifically, O1 hydroxyl oxygen, C2 benzoyl oxygen and O2' hydroxyl oxygen are not interacting with any tubulin residues, but are free to form hydrogen bonds with either solvent or other Taxol molecules, possibly allowing the formation of Taxol crystal lattice (Fig. 5c).

The predicted Taxol-binding site should not affect the interaction between β and α subunits. On the other hand the site is directly on the side of the α - β dimer that is responsible for lateral interactions with another subunit and may interfere with lateral contacts between assembling tubulin dimers probably preventing MT growth. There is no overlap between the native and the new binding site, since they are separated by approximately 30 Å. We predict in our previous work [14] that the “native” site has two times higher affinity to Taxol than the secondary site. This latter site may therefore possibly bind Taxol only at a high Taxol concentration, when the “native” sites within all microtubules are saturated. In the case of MTs, the geometry of this secondary site may be altered due to interactions with other tubulin subunits; hence this alternative binding site may not be functional in the MT. This could explain our experimental observation of why MTs do not nucleate Taxol spherulites.

As explained before, Taxol spherulites nucleated from tubulin are formed in a tubulin-containing solution when Taxol is added above its saturation limit. Based on all the data we have gathered we can hypothesize that the nucleus formation of Taxol spherulites is plausible. The high Taxol concentration in the tubulin-containing solution can lead to the formation of nuclei composed of Taxol–tubulin complexes, probably more disordered than tubulin oligomers or MTs, interacting through the secondary Taxol-binding site. In the center of each spherulite there are multiple heterodimers, that start growth of Taxol crystals. Each heterodimer is most likely responsible for growing a single Taxol needle. The growth of Taxol needles takes place in all directions due to the disordered structure of nucleation center of the spherulite.

3. Conclusions

Taxol crystallization was studied in water and tubulin-containing aqueous solutions. Taxol crystallizes spontaneously when it is mixed with aqueous solutions above its solubility limit of 0.77 μM [15]. Furthermore, we found that Taxol crystals can be formed by homogeneous and heterogeneous nucleation, displaying different morphologies, which are in accordance with their description presented in other investigations [20]. Taxol crystals obtained by homogeneous nucleation takes on the morphology of axialites (sheaf-like structures) without a defined nucleus whereas those formed by heterogeneous nucleation, using tubulin as nucleating agent displayed very symmetrical and spherical shapes (spherulites) with well defined cores. In addition, Taxol spherulites nucleated from tubulin were also grown in tubulin-containing gels. These gels simulate the cytoplasm environment suggesting the possibility for free tubulin in the cytoplasm to trigger nucleation of Taxol spherulites when Taxol accumulates within the cell to concentrations exceeding its solubility limit. Based on

previous computational studies [14] and on the experimental evidence reported here, we proposed that heterogeneous nucleation of Taxol spherulites due to tubulin is made possible by the presence of a secondary Taxol-binding site in the tubulin dimer. This new potential Taxol-binding site could add a novel tubulin–Taxol interaction in the cell, where tubulin may nucleate Taxol crystals for Taxol concentrations exceeding its saturation limit (which is very low). In addition, we have demonstrated, experimentally and theoretically, that Taxol crystals have exposed functional groups in their surface that may strongly interact with a variety of other molecules [14] leading to yet unknown biological activities. It is interesting to note that the results presented in this work may have direct impact on the therapeutic use of Taxol as an anti-cancer agent. Besides the known ability of Taxol to stabilize MTs, the probable ability of tubulin dimers to nucleate Taxol crystals in the cytoplasm should also be considered. We can suggest several ways in which Taxol crystallization may affect cell functions. First, therapeutic efficacy of Taxol could be highly dosage sensitive in as yet undetermined ways since Taxol molecules could be forming crystals in addition to interacting with MTs. Even if Taxol is dosed below its solubility limit ($0.77 \mu\text{M}$ [15]) intracellular concentrations can surpass this value [26]. Second, the presence of Taxol crystals within the cell may alter its physiology due to the potential interactions with a variety of molecules/proteins in the cytoplasm. It is possible, that formation of Taxol crystals may be also used for a therapeutic purpose, e.g., for triggering apoptosis by interacting with the Bcl-2 anti-apoptotic protein [27] if the crystals could be targeted to a subset of non-dividing, dysfunctional cells.

In addition, the potential heterogeneous nucleation of Taxol can raise some questions regarding the established mechanisms of interaction and anti-mitotic effect of Taxol in cells. In a number of studies Taxol has been reported to induce cytoplasmic MTs asters in cells treated with the drug [e.g., [9,10,28,29]]. Most of these studies have used Taxol concentrations above $0.77 \mu\text{M}$ and have been observed by fluorescent microscopy. A simple morphological inspection of MTs asters reported in these studies allows us to think that at least some of them can be Taxol crystals nucleated heterogeneously. In this case heterogeneous nucleation involves sequestration of tubulin in the cytoplasm, which could significantly limit the availability of tubulin for mitotic spindle formation depending on the cell cycle stage during which crystal formation occurred. Thus, cell division would be affected not only by MTs stabilization but also by tubulin depletion.

Furthermore, while Taxol stabilization of MT spindles may still be the primary mechanism for apoptosis of fast-dividing cancerous cells, crystallization of Taxol crystals may disrupt non-dividing healthy cells. Taxol-induced cytotoxicity by crystallization in non-dividing cell may be the cause of serious side effects that could reduce the efficacy of Taxol-based cancer treatments.

4. Materials and methods

4.1. Materials

The following materials were used: PEM80 buffer (80 mM PIPES, 0.5 mM EGTA, 4 mM MgCl_2), paclitaxel (Taxol) dissolved in DMSO at 2 mM, fluorescent rhodamine tubulin from bovine brain (cat. #T331 M), tubulin protein from bovine brain (Cat. # TL238), and guanosine 5' triphosphate (GTP). All these materials were purchased from Cytoskeleton®. We also used Tetramethylrhodamine (TMR) (cat. # C1171) obtained from Invitrogen® and a low gelling temperature agarose [ultra pure Agarose low melting point, gelling temperature (2 wt%) 26–30 °C] obtained from Gibco-brl Life technologies®.

4.2. Preparation of MT supporting buffer

GTP diluted in PEM80 buffer at a concentration of 1 mM.

4.3. Taxol axialites formed in pure water

On an ice bath Taxol was diluted in MT supporting buffer to a final concentration of $100 \mu\text{M}$, the solution was vortexed and incubated for 30 min at room temperature to obtain a complete Taxol crystallization.

4.4. Fluorescent labeling of Taxol spherulites with rhodamine

The Rhodamine was added to a solution containing Taxol spherulites. Rhodamine final concentration was $5 \mu\text{M}$. Subsequently the solution was incubated during 20 min at room temperature.

4.5. Taxol spherulites formed in tubulin-containing solution

On an ice bath the tubulin (pure tubulin or rhodamine tubulin) was added to the MT supporting buffer to a concentration of $9.1 \mu\text{M}$, immediately Taxol was added to a final concentration of $100 \mu\text{M}$, the solution was mixed and incubated for 30 min at room temperature.

4.6. Taxol spherulites formed by diffusion in tubulin-containing gel

Gel samples were prepared using a solution of agarose (0.5 wt%) in MTs supporting buffer. The solution was boiled and then cooled to 31 °C and maintained at this temperature in a liquid state. To this, tubulin rhodamine was added and mixed to a final concentration of $9.1 \mu\text{M}$. The tubulin agarose solution was used to partially fill a rectangular column. The rectangular column (5 mm × 1.5 mm × 10 mm) with optically transparent walls was filled with $20 \mu\text{L}$. The column was cooled to 4 °C for 10 min in order to solidify the gel and prevent or slow further assembly of MTs. After that $15 \mu\text{L}$ of Taxol was deposited on the surface of the gel. The sample was incubated at room temperature for 30 min while the Taxol diffused through the gel. The sample was analyzed few minutes after its preparation.

4.7. Fluorescent microscopy

The fluorescent samples were observed in an Olympus inverted fluorescent microscope model IX71 using excitation emission of 494 nm for the Rhodamine. The images were taken with a 100× oil lens and a 40× lens.

4.8. DIC microscopy

The samples were analyzed in a Nikon eclipse TE200 microscope using 100× oil lens. Images were recorded in a VHS cassette and digitalized for the extraction of images.

Acknowledgements

We acknowledge financial support from NSF/NIRT Grant 0303863.

We thank K. Visscher from the department of Physics for access to his DIC microscope, S. Klewer, Department of Pediatrics, for access to his laboratory.

References

- [1] E.K. Rowinsky, R.C. Donehower, *New Engl. J. Med.* 332 (1995) 1004.
- [2] E.K. Rowinsky, L.A. Cazenave, R.C. Donehower, *J. Natl. Cancer Inst.* 82 (1990) 1247.
- [3] M.C. Wani, H.L. Taylor, M.E. Wall, P. Coggon, A.T. McPhail, *J. Am. Chem. Soc.* 93 (1971) 2325.
- [4] T.H. Wang, H.S. Wang, Y.K. Soong, *Cancer* 88 (2000) 2619.
- [5] M.A. Jordan, L. Wilson, *Nat. Rev. Cancer* 4 (2004) 253.
- [6] J. Szebeni, C.R. Alving, S. Savay, Y. Barenholz, A. Priev, D. Danino, Y. Talmon, *Int. Immunopharmacol.* 1 (2001) 721.
- [7] N.I. Marupudi, J.E. Han, K.W. Li, V.M. Renard, B.M. Tyler, H. Brem, *Expert Opin. Drug Saf.* 6 (5) (2007) 609.
- [8] Q.Y. Sun, L. Lai, G.M. Wu, K.W. Park, B.N. Day, R.S. Prather, H. Schatten, *Mol. Reprod. Dev.* 60 (2001) 481.
- [9] F. Verde, J.M. Berrez, C. Antony, E. Karsenti, *J. Cell. Biol.* 112 (1991) 1177.
- [10] G. Callaini, M.G. Riparbelli, *Cell Motil. Cytoskel.* 37 (1997) 300.
- [11] O.V. Zatsepina, A. Rousselet, P.K. Chan, M.O. Olson, E.G. Jordan, M. Bornens, *J. Cell Sci.* 112 (1999) 455.
- [12] H. Nilsson, M. Wallin, *Cell Motil. Cytoskel.* 41 (1998) 254.
- [13] M. Foss, B.W. Wilcox, C.G. Alsop, D. Zhang, *PLOS One* 3 (2008) e1476.
- [14] J.S. Castro, B. Trzaskowski, P.A. Deymier, J. Bucay, L. Adamowicz, J.B. Hoying, *Mater. Sci. Eng. C* (2009), doi:10.1016/j.msec.2008.12.026.
- [15] R. Shi, H.M. Burt, *Int. J. Pharm.* 271 (2004) 167.
- [16] M.C.R. Heijna, M.J. Theelen, W.J.P. van Enckevort, E. Vlieg, *J. Phys. Chem. B* 111 (2007) 1567.
- [17] P.S. Chow, X.Y. Liu, J. Zhang, R.B.H. Tan, *Appl. Phys. Lett.* 81 (11) (2002) 1975.
- [18] K.R. Domike, A.M. Donald, *Biomacromolecules* 8 (2007) 3930.
- [19] H.M. Cuppen, A.R.T. van Eerd, H. Meekes, *Cryst. Growth Des.* 4 (2004) 989.
- [20] P. Philips, *Handbook of Crystal growth*, vol. 2, Elsevier, Amsterdam, 1993 (Chapter 18).
- [21] E. van Veenendaal, P.J.C.M. van Hoof, J. van Suchtelen, W.J.P. van Enckevort, P. Bennema, *Surf. Sci.* 417 (1998) 121.
- [22] F. Puel, E. Verdurand, P. Taulelle, C. Bebon, D. Colson, J.P. Klein, S. Veessler, *J. Cryst. Growth* 310 (2008) 110.
- [23] J.S. Castro, P.A. Deymier, S.D. Smith, J.B. Hoying, *Adv. Mater.* 20 (2008) 183.
- [24] J.P. Snyder, J.H. Nettles, B. Cornett, K.H. Downing, E. Nogales, *Proc. Natl. Acad. Sci. U.S.A.* 98 (2001) 5312.
- [25] D. Mastroaolo, A. Camerman, Y. Luo, G.D. Brayer, N. Camerman, *Proc. Natl. Acad. Sci. U.S.A.* 92 (1995) 6920.
- [26] A.M. Yvon, P. Wadsworth, M.A. Jordan, *Mol. Biol. Cell* 10 (1999) 947.
- [27] D.J. Rodi, R.W. Janes, H.J. Sanganee, R.A. Holton, B.A. Wallace, L. Makowski, *J. Mol. Biol.* 285 (1999) 197.
- [28] T. Gaglio, A. Saredi, D.A. Compton, *J. Cell Biol.* 131 (3) (1995) 693.
- [29] M.A. Dionne, A. Sanchez, D.A. Compton, *J. Biol. Chem.* 275 (16) (2000) 12346.